JOURNAL OF MATERIALS SCIENCE 24 (1989) 717–725

Y(Er)-doped tetragonal zirconia polycrystalline solid electrolyte

Part 3 *Electrical properties*

P. DURÁN, P. RECIO, J. R. JURADO, C. PASCUAL, M. T. HERNANDEZ, C. MOURE
Departamento de Materiales Cerámicos Especiales, Instituto de Cerámica y Vidrio (CSIC), Arganda del Rey, Madrid, Spain

The electrical conductivity of fully dense bodies of polycrystalline tetragonal zirconia (TZP) in the composition range 2 to 3 mol % Y_2O_3 (Er_2O_3) was measured.Throughout this work, a.c. impedance complex plane analysis was used. From this method grain-interior and grain-boundary conductivity contributions were obtained separately. Plots of conductivity against reciprocal temperature of both contributions were evaluated. An electrode–electrolyte interphase conductivity contribution was detected and considered. The influence of impurities, and ageing behaviour was also studied. The activation, migration and association energies were estimated and discussed on the basis of up-to-date theoretical and structural information.

1. Introduction

At the beginning of the 1980s a great deal of interest spread through the ceramic scientific world, provoked by the potential possibilities of tetragonal zirconia polycrystalline (TZP) material as a structural ceramic. Still today an extensive number of publications deal with the preparation and properties of such substances. A state of the art assessment and detailed information from our own studies concerning the powder fabrication and processing routes involved, were given in Part 1 [1]. A survey of microstructure and mechanical behaviour was extensively discussed in Part 2 [2]. Erbia-doped tetragonal polycrystalline zirconia was also fabricated in order to compare its behaviour as a high technical ceramic with the yttria-doped TZP.

Electrical properties have not received the same interest, however, a number of papers [3–11] devoted to this topic have been published. From its relevant room temperature mechanical properties, TZP has also basically considered as a structural material (with potential applications in the car industry), rather than a solid electrolyte to use in oxygen sensors or in fuel-cell devices. Nevertheless, due to its confirmed high ionic conductivity at low-temperature, it challenges other traditional solid electrolytes. On the other hand, TZP ceramics, we believe, are not such excellent materials as previously considered: various significant problems indicate that its potential for industrial applications is now seriously doubted, not only as a structural ceramic but also as a solid electrolyte. However efforts to overcome such difficulties involve determining how a tetragonal matrix can enhance its ageing behaviour and reduce the metastability temperature.

One alternative is to incorporate into the tetragonal matrix adequate amounts of CeO_2 or Al_2O_3 [12–14]. In both cases, but particularly after the CeO_2 introduction, the ageing behaviour was really improved [14] and, as expected, CeO_2 seems to lower the metastability temperature of the tetragonal phase according to phase diagram assumptions [15, 16].

This paper describes a general scope of electrical conductivity behaviour with special emphasis on impedance spectroscopy studies, of the Y(Er)-TZP materials, and discusses all the relevant data available. Finally, some preliminary results on electrical conductivity of a Y-TZP ceramic containing CeO_2 are given.

2. Experimental work

Powder processing and sintering behaviour have been extensively described in Parts 1 and 2 [1, 2]. Electrical conductivity data were taken from selected samples with high-density (~98% theoretical density) pure tetragonal phase with very uniform microstructure, and a careful control of impurities.

A systematic work, although necessary, is very complicated, and no attempt was made to correlate property density evolution, microstructure and grain morphology with electrical parameters, because electrical characterization alone needs control of a number of important variables to ensure reproducible and reliable measurements. For instance, one of the most relevant factors to take into account is the contact electrodes; we have used different electrodes, and platinum (sputtered or paste) and silver paste have been basically employed throughout the experiments performed.

Electrical conductivity data were attained using a.c. impedance complex plane spectra over a frequency range 5 to 10^7 Hz in the temperature interval of 200 to 500° C; when it was necessary to extend this temperature range to higher experimental temperatures (i.e. up to 900° C), measurements were taken carefully,

0022–2461/89 $03.00 + .12

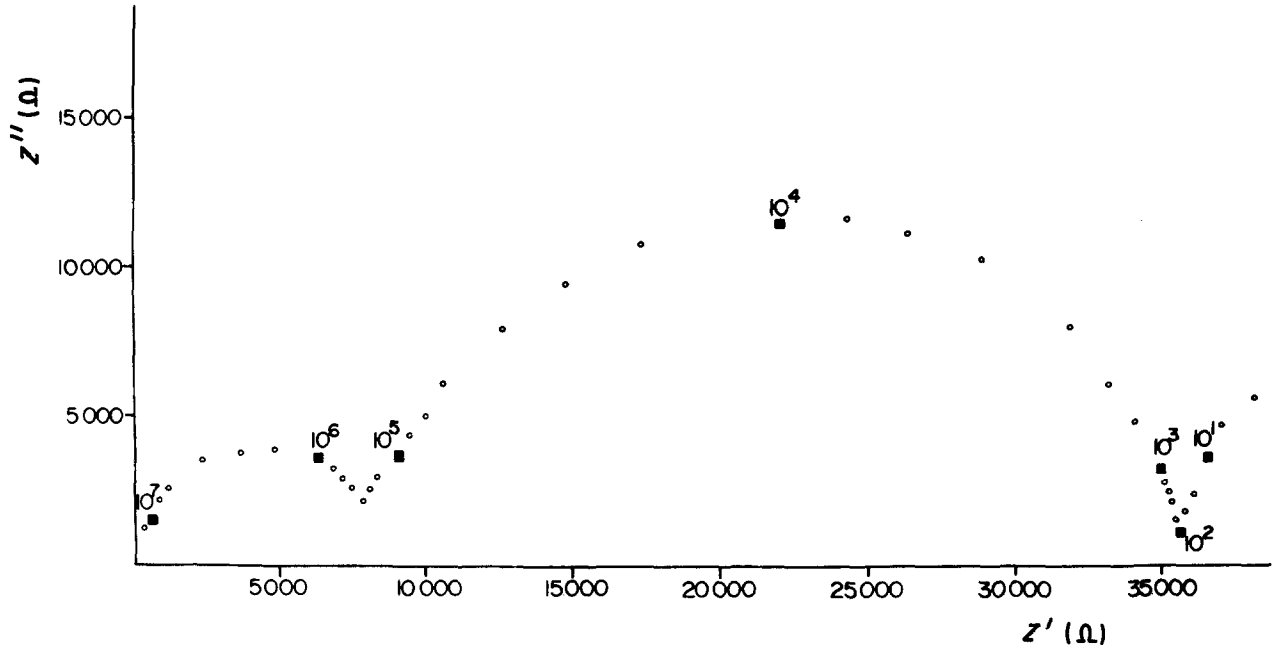

Figure 1 A.c. impedance plots of 3 mol % Y_2O_3–TZP, 300° C.

because at those temperatures serious electrode alterations are produced. To avoid electrode polarization, voltages of 20 to 200 mV were applied to the two terminal contacts. A Hewlett-Packard impedance analyser model 4192 A connected to a computer interphase HP model 9000-216 were utilized. Experiments were carried out in an air atmosphere and data were taken after strict temperature control of the hot sample holder. In order to detect the possible effect of the tetragonal to monoclinic transformation on the electrical measurements, the data during heating and cooling were collected.

3. Results

In spite of their low dopant concentration, tetragonal zirconias exhibit an unexpected high electrical conductivity, particularly in the temperature range 200 to 500° C; unfortunately the electrical behaviour of TZPs has received little attention and therefore specific information on oxygen partial pressure ionic domain and *in situ* electric ageing tests are still scarce. In the present work we are only concerned with the impedance complex plane measurements and studying the influence of various factors which could affect the electrical performance of TZP ceramics; for instance: impurity concentration, Y_2O_3 replacements by Er_2O_3, the experimental regime (cooling–heating), and *in situ* electrical ageing tests.

According to Bauerle [17] impedance spectra become useful tools to characterize basically fluorite-

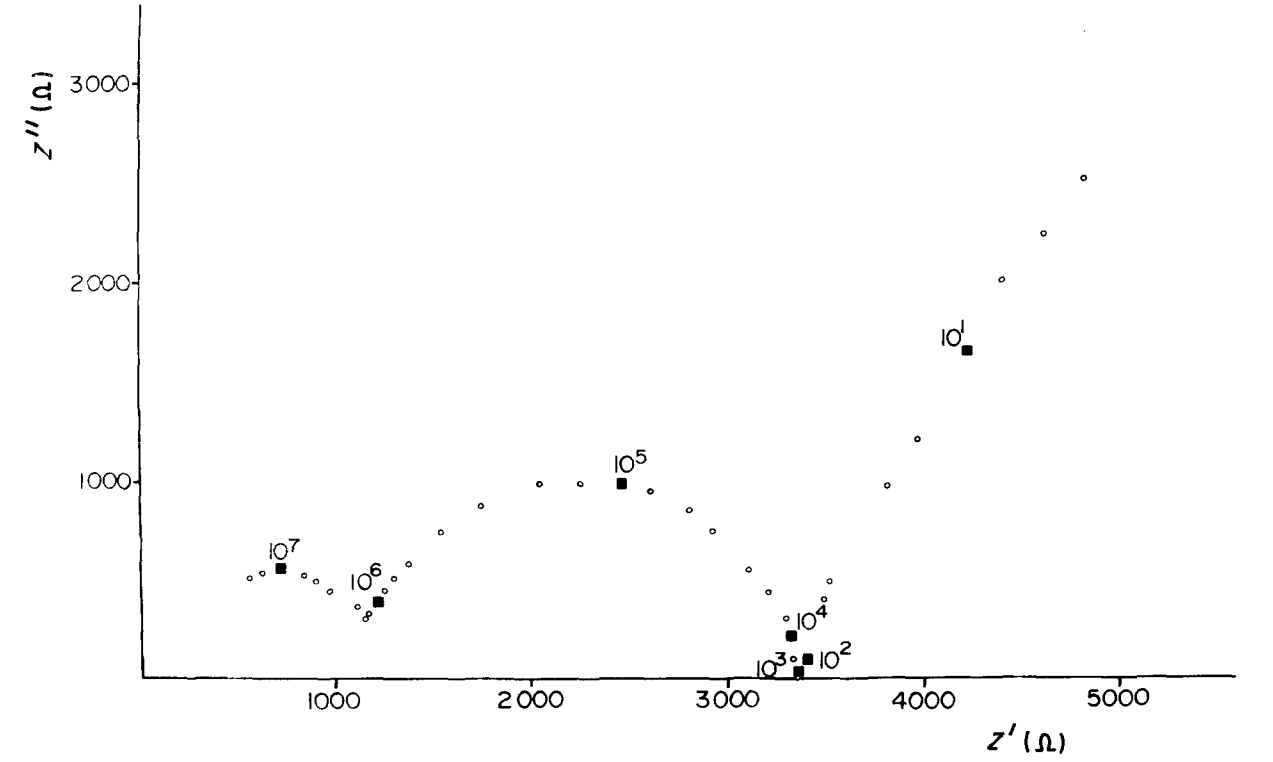

Figure 2 A.c. impedance plots of a 3 mol % Y_2O_3–TZP ceramic, 400° C.

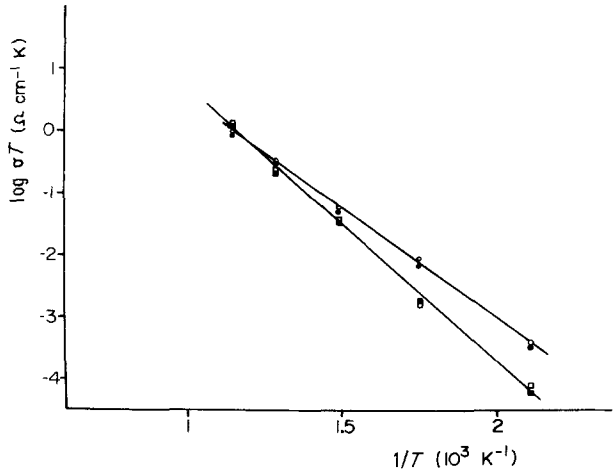

Figure 3 Log σ as a function of reciprocal temperature over several cooling-heating cycles. (●) Bulk (heating), (■), GB, (○) bulk (cooling), (□) GB.

related zirconias. In fact, the effect of separated resistance contributions in a ceramic body (in our TZPs), i.e. grain interior, grain-boundary and electrode–electrolyte interphase resistances, are perfectly illustrated in the impedance spectrum shown in Fig. 1. This is a representative example of a highly dense (> 98% theoretical density) 3% Y_2O_3–TZP ceramic. The three arcs that subsequently arise when frequency is varied, correspond to grain-interior (high-frequency arc), grain-boundary (intermediate frequency arc), and electrode–electrolyte interphase (low-frequency arc) respectively. All semicircles have a depression angle < 10°, which means that the electrical conductivity and/or the dielectric properties of TZP are rather dispersed. The presence of these arcs is evidence that a high-purity ionic conductivity is produced; the same picture can be seen in Fig. 2 when the temperature is raised. However, a larger electrode–electrolyte interphase arc indicates that at higher temperatures (> 500° C), the electrode–electrolyte interphase can become a straight line implying that other possible conducting species, distinct from ionic ones, will modify that spectrum as expected. This fact could involve a limitation of use of this material in fuel-cell devices, particularly at temperatures as high as 800° C. Nevertheless, prior to drawing any conclusions, it is very important to set up appropriate experiments for conductivity–oxygen partial pressures as the temperature is varied. Furthermore, platinum catalytic electrodes undergo a strong degradation at temperatures higher than 600° C. Following the results of Mari [18], we attempted to use, as catalytic electrodes, a number of perovskite and relate materials, whose electrode behaviour is now very promising.

To investigate the stability of the tetragonal phase in our samples, we have designed experiments where specimens for electrical measurements have remained for at least a week inside the hot sample holder; they underwent a number of thermal cycles (heating and cooling) and impedance data were taken from time to time, to test how the TZP stands up to temperatures in the range 200 to 500° C. It is known that around 200° C TZP is degraded and a strong and dramatic tetragonal–monoclinic transformation takes place. Fig. 3 shows the conductivity–reciprocal temperature curves of a Y-TZP which underwent thermal treatments. It is observed that no evidence of changes or impedance modifications was detected and consequently grain-boundary and grain-interior conductivities basically do not change. After the cyclic heat treatment the sample was removed from the hot-sample holder and X-ray diffraction indicated that the stable tetragonal crystalline phase was maintained and no monoclinic phase was detected. These experiments are not conclusive; however, an idea was formed about how constraint tetragonal matrix was achieved and retained. In order to test the real stability performance, more aggresive environment experiments are now in progress.

When Y_2O_3 is totally replaced by Er_2O_3 it is normally supposed that, because of the electronic

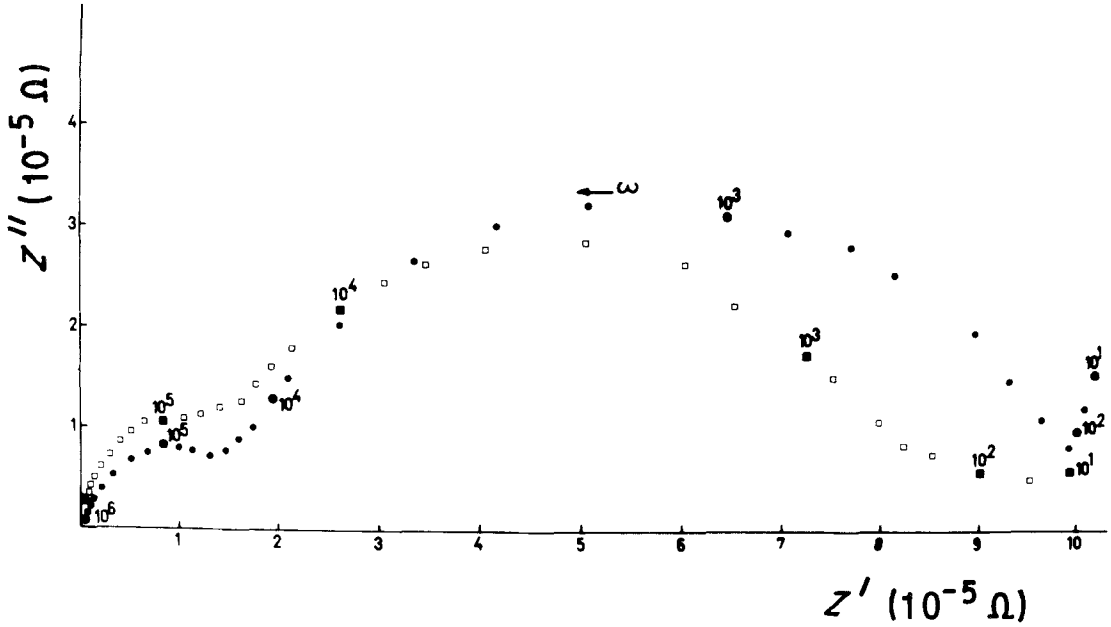

Figure 4 A.c. impedance plots of Er_2O_3-doped TZP ceramic. T = 300° C (●) TZP-Er1 – 97% ZrO_2–3% Er_2O_3, 1600° C, 6 h. (□) TZP-Er2 – 97% ZrO_2–3% Er_2O_3, 1420° C, 1 h.

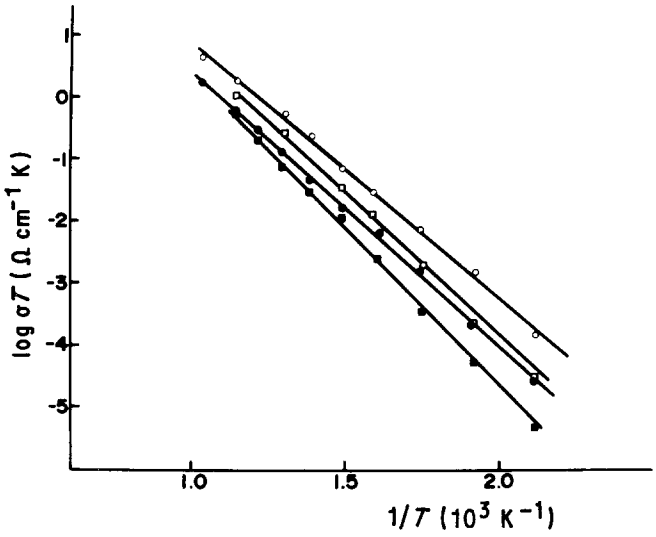

Figure 5 Log σ plotted against reciprocal temperature of various Y(Er)-TZP ceramics. TZP-Y1 – 97% ZrO_2–3% Y_2O_3, 1600° C, 6 h. TZP-Er1 – 97% ZrO_2–3% Er_2O_3, 1600° C, 6 h. (○) Bulk TZP-Y1, (●) bulk TZP-Er1. (□) GB TZP-Y1, (■) GB TZP-Er1.

structure of the erbium ion, the vacant concentration when ZrO_2 or other oxides are doped with Er_2O_3 should be slightly higher than those doped with Y_2O_3, and therefore Er-TZP should have slightly higher conductivity than Y-TZP. Unfortunately, there are few reports in the literature on Er-doped zirconias; only Won *et al.* [19] have reported an extensive study on electrical conductivity of the free tetragonal ZrO_2–Er_2O_3 region. They have measured d.c. electrical conductivity as a function of oxygen partial pressure, and observed two temperature regions in the conductivity plots. At 400 to 650° C the ionic conductivity predominates and conduction is by the diffusion of an oxygen ion to an oxygen vacancy. They noted a conductivity decrease as the dopant level of erbia increased, suggesting it is due to an order-disorder transition. At 600 to 1000° C a mixed electronic conduction, due to oxygen ions and electrons, can take place. At 400° C, Won *et al.* found for the composition 10 mol % Er_2O_3–ZrO_2 a conductivity of $\sim 5.60 \times 10^{-6}\,\Omega\,cm^{-1}$, while for a composition 10 mol % Y_2O_3–FSZ at the same temperature the conductivity is $\sim 6.8 \times 10^{-5}\,\Omega\,cm^{-1}$, which is clearly higher.

These authors have not investigated the electrical conductivity of Er-TZP compositions, and therefore our data are the only results published in the literature consulted to date. However, we have observed the same electrical behaviour, i.e. the conductivity of Er-TZP is always slightly lower than Y-TZP.

Fig. 4 depicts the impedance plot of Er-TZP ceramics; if compared with Y-TZP ceramic (Figs 1 and 2) a tendency to overlapping of both grain-interior and grain-boundary arcs can be seen, a behaviour which is less significant in Y-TZP or in other solid electrolytes and could be related to the influence of the electrode–electrolyte interphase on the total equivalent circuit involved. The large grain-boundary arc in shape and in magnitude is very similar to the Y-TZP bodies. Bulk and grain boundary intercept resistances on the Z' axis are taken to draw the conductivity as a function of reciprocal temperature in Fig. 5.

The Arrhenius plots of the bulk- and grain-boundary conductivities were linear over the temperature range investigated. The values of conductivity at 300° C and the activation enthalpy for both bulk- and grain-boundary conductivities of all samples are listed in Table I; corresponding values obtained for PSZ, FSZ and TZP reported by Bonanos *et al.* [4] are also given for comparison. It can be observed that Er-TZP ceramics show a very high conductivity and have similar (slightly lower) values than the PSZ and FSZ ceramics; moreover they have lower activation enthalpy which is considered to be promising electrical behaviour.

When the dopant concentration is lowered from 3 to 2 mol % Y(Er_2O_3) the electrical conductivity does not change significantly, as can be seen in Figs 6 and

TABLE I Electrical characteristics of several zirconia solid solutions

Sample	σ_{300}(B) ($S\,cm^{-1}$)	σ_{300}(GB) ($S\,cm^{-1}$)	ΔH(B) (eV / $kJ\,mol^{-1}$)	ΔH(GB) (eV / $kJ\,mol^{-1}$)
Y-TZP	1.11×10^{-5}	3.41×10^{-6}	0.82 79.0	0.98 94.4
Er-TZP	2.59×10^{-6}	5.67×10^{-7}	0.88 84.8	1.02 98.2
TZP [4]	7.70×10^{-6}	1.64×10^{-6}	0.92 88.6	1.09 105.0
PSZ 4.7% Y_2O_3 [4]	3.85×10^{-6}	7.14×10^{-6}	1.07 103.1	1.15 105.0
FSZ 6.0% Y_2O_3 [4]	5.56×10^{-6}	1.25×10^{-5}	1.07 103.1	1.12 107.9

B = bulk. GB = grain boundary.

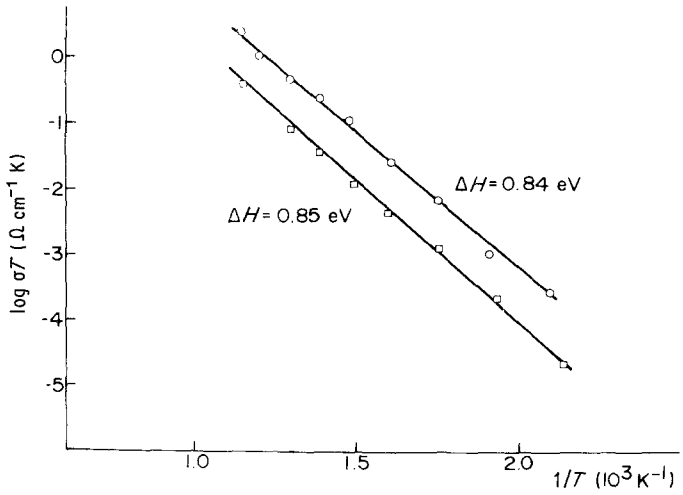

Figure 6 Log lattice conductivity plotted against $1/T$ of Er-TZP ceramics. (○) Bulk TZP-2% Er_2O_3; (□) bulk TZP-3% Er_2O_3.

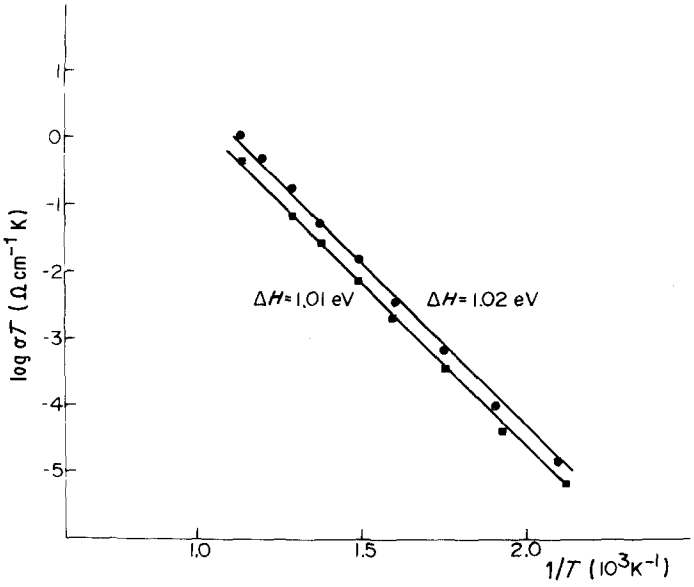

Figure 7 Log grain-boundary conductivity plotted against reciprocal temperature of Er-TZP ceramics. (●) GB TZP-2% Er_2O_3, (■) GB TZP-3% Er_2O_3.

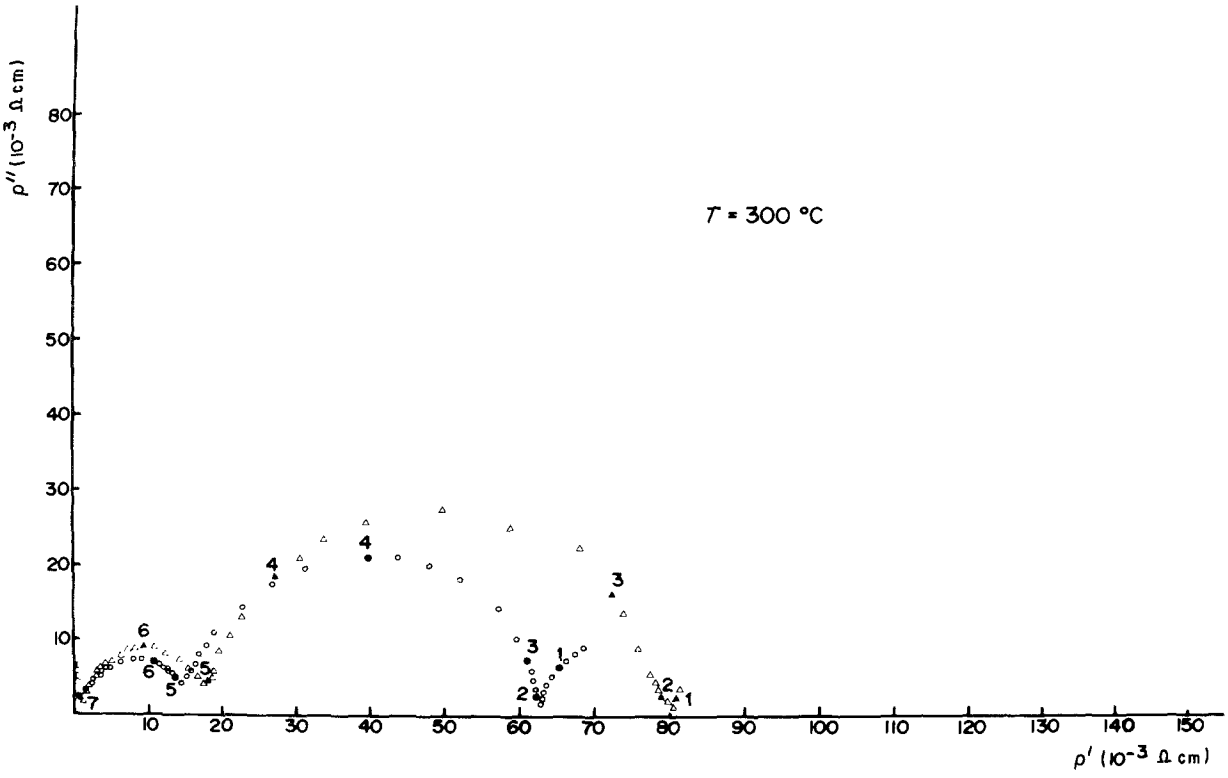

Figure 8 A.c. impedance plots of two 3 mol % Y_2O_3–TZP ceramics 1, (△) white sample; (○) black sample, 1550° C, 6 h.

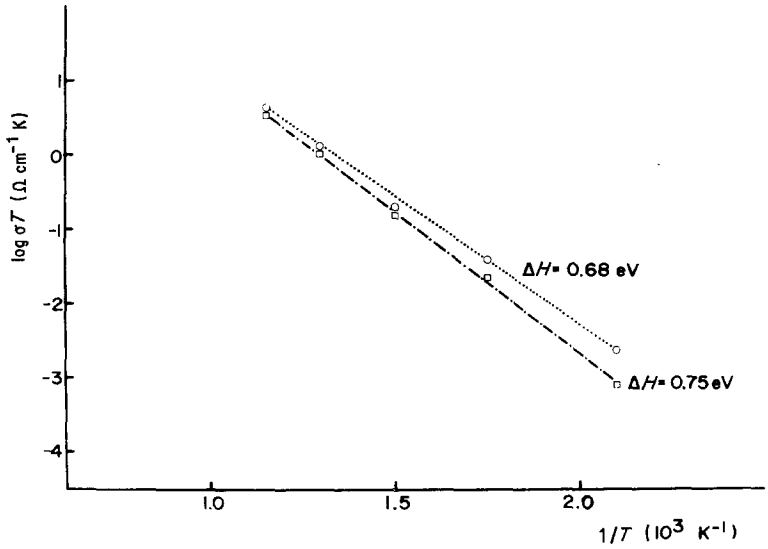

Figure 9 Log grain-interior conductivity plotted against reciprocal temperature of the (□) white and (○) black samples.

7; it can involve the "free" vacancy concentration remaining constant as the doped ion concentration falls. We have even found a slightly higher conductivity for 2 mol % Er_2O_3 ($1.2 \times 10^{-5} \Omega cm^{-1}$) than for 3 mol % [7]. When the Y_2O_3 proportion was lowered, the conductivity hardly changed. Erbia-doped TZP shows that the activation enthalpy for conduction does not significantly change, whether processing is by doping level and/or impurity concentration; this can be explained by the fact that the vacancy ordering in Er-TZP is more stable than in Y-TZP, which indicates a stable TZP structure when ZrO_2 is doped by Er_2O_3. On the other hand, in Y-TZP samples we have found a strong tendency to modification of their electrical properties when certain ceramic parameters are varied; an example of this behaviour can be observed in Fig. 8 where a 3 mol % Y_2O_3–TZP is shown which exhibits a blackening phenomenon, due probably to the presence either a transition metal ion (Fe) or alumina in the composition. This sample exhibits the highest conductivity value and the lowest activation enthalpy compared with the rest of our specimens. Arrhenius plots of log σT against $1/T$ (Figs 9 and 10) were linear over the explored temperature range (200 to 500° C). The low activation enthalpy for conduction when an aliovalent ion is introduced into the batches might imply that Y-TZP can undergo easy structural modifications which allow the mean free path for the oxygen vacancy motion to increase. In conclusion, from these results, network distortion in the oxygen sublattice, when specific impurities are introduced, can be expected. However, Keizer *et al.* [6, 9] have not detected any structural distortion in their TZP; therefore, they have suggested that the high electrical conductivity observed in such materials is governed by other mechanisms.

Finally, Fig. 11 describes the classical impedance spectrum of the three selected highly densified ceramic solid electrolytes compared with other ionic solid electrolytes prepared by us. Stabilized bismuth oxides doped with Er_2O_3 show the highest conductivity at the highest temperature as it shown in Fig. 12 and Table II. From these results one can infer that CeO_2–Gd_2O_3 materials would be the best oxygen ionic conductor at low temperatures; however, cerium-related ceramics exhibit serious oxidation–reduction problems and erbia-doped bismuth oxides are very expensive and have too high an activation enthalpy for conduction; therefore Y-TZP can compete with these if its ageing effect and electrical response in aggressive environmental conditions are overcome.

We are now preparing Y-TZP ceramics from the

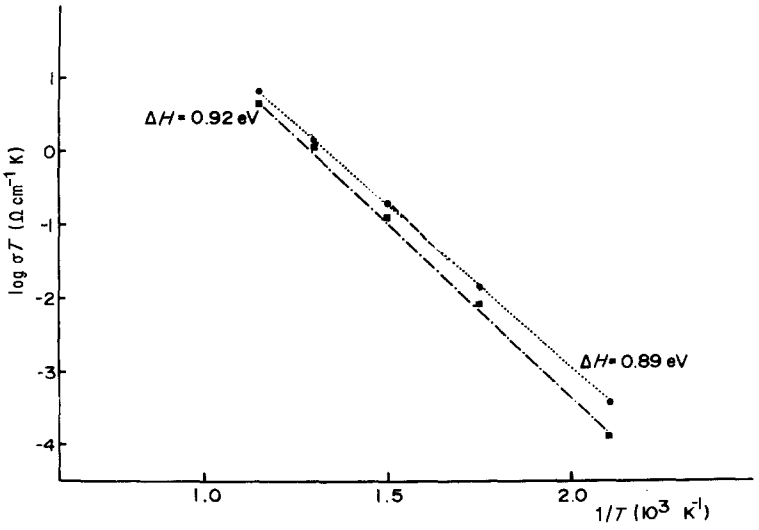

Figure 10 Log grain-boundary conductivity as a function of temperature of (●) the black and (■) white Y_2O_3–TZP samples.

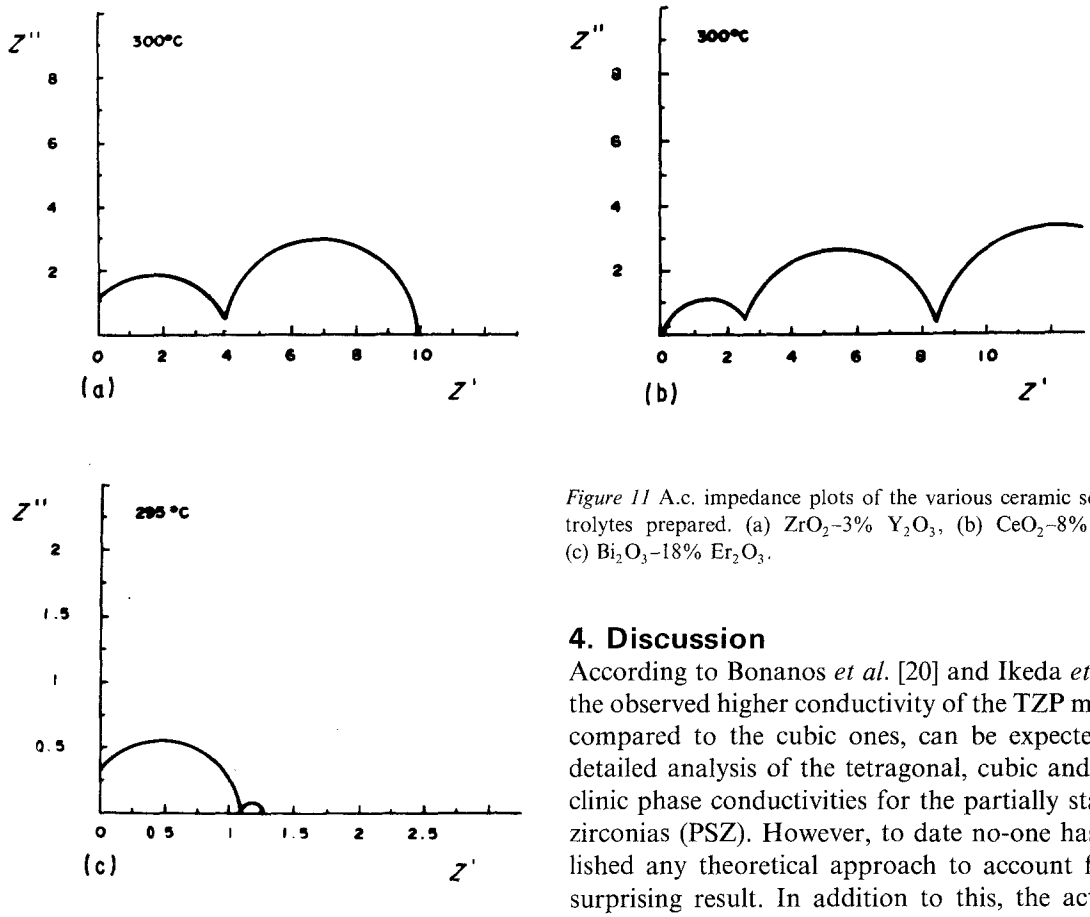

Figure 11 A.c. impedance plots of the various ceramic solid electrolytes prepared. (a) ZrO_2–3% Y_2O_3, (b) CeO_2–8% Gd_2O_3, (c) Bi_2O_3–18% Er_2O_3.

composition range 1.7 to 3 mol 3% Y_2O_3 by introducing into the batches, proportions of CeO_2 as high as 10 mol %. Tsakuma and Shimada [14] had reported a significant reduction in the tetragonal–monoclinic transformation on the incorporation of adequate amounts of CeO_2 and Al_2O_3 into the TZP matrix; the ageing response is substantially improved.

Our preliminary results indicate that a stable Y-TZP crystalline phase was achieved, with an average grain size of 0.7 μm and a relative density of $\geqslant 95\%$ theoretical density. Fig. 13 shows the impedance plot of the 3 mol % Y_2O_3–TZP with 10 mol % CeO_2. Bulk and grain boundary arcs are observed and the second one exhibits a smaller size compared with semicircles obtained in pure Er(Y)-TZP (see Figs 1, 5); this is an interesting result, because to reduce the grain-boundary effect is one of the most important objectives currently found in the literature.

It can be expected that CeO_2 may be segregated in the boundaries and consequently it could induce better electrical conductivity response in those regions.

Table III shows that, as CeO_2 is incorporated into the Y-TZP matrix, the electrical conductivity decreases and activation enthalpy increases. At the present time, further work is being done to determine the appropriated amount of CeO_2 required to retain the high level of electrical parameters of typical TZP.

4. Discussion

According to Bonanos *et al.* [20] and Ikeda *et al.* [21] the observed higher conductivity of the TZP materials compared to the cubic ones, can be expected from detailed analysis of the tetragonal, cubic and monoclinic phase conductivities for the partially stabilized zirconias (PSZ). However, to date no-one has established any theoretical approach to account for that surprising result. In addition to this, the activation energy for conduction for grain-interior and grain-boundary contributions is smaller than in zirconia fluorite materials.

It is now accepted that the conductivity pattern in solid electrolyte ceramic systems is governed by the activation energy for conduction, ΔH_σ, which contains two terms $\Delta H_\sigma = \Delta H_m$ (ionic migration enthalpy) + ΔH_{AI} (association enthalpy). We are using the usual meaning of the terms.

ΔH_{AI} is the association enthalpy of the oxygen vacancies trapped by dopant M^{3+} cations, as it is known that this pair formation reduces the "free" vacancy concentration. It is therefore accepted that low ΔH_{AI} values imply a better electrical conductivity, so when the activation enthalpy for conduction, ΔH_σ, is lowered, it is due either to a reduction in ΔH_m, ΔH_{AI} or in both of these parameters. Unfortunately, no data are available concerning any theoretical calculation on pure tetragonal structure, in order to obtain ΔH_m [22, 23]. Bauerle and Hrizo [24] have obtained $\Delta H_m = 0.68$ eV in FSZ samples. This value has been widely accepted and it was estimated taking into account experimental conductivity data, and a break in the Arrhenius plots was detected. In a recent work, Weller and Schubert [10] have reported mechanical and dielectric relaxation experiments. They have also detected in the conductivity curve a break at 790 K (527° C) and they assumed that conduction at higher

TABLE II Some electrical parameters of various solid electrolytes

Sample	$\sigma_{300}(\Omega\,cm^{-1})$	σ_{500}	σ_{700}	ΔH(kcal mol^{-1})
ZrO_2–3% Y_2O_3	1.02×10^{-5}	3.24×10^{-4}	1.59×10^{-3}	65.3
CeO_2–8% Gd_2O_3	3.89×10^{-4}	5.25×10^{-3}	3.31×10^{-2}	66.0
Bi_2O_3–18% Er_2O_3	4.80×10^{-5}	5.89×10^{-2}	2.14	129.6

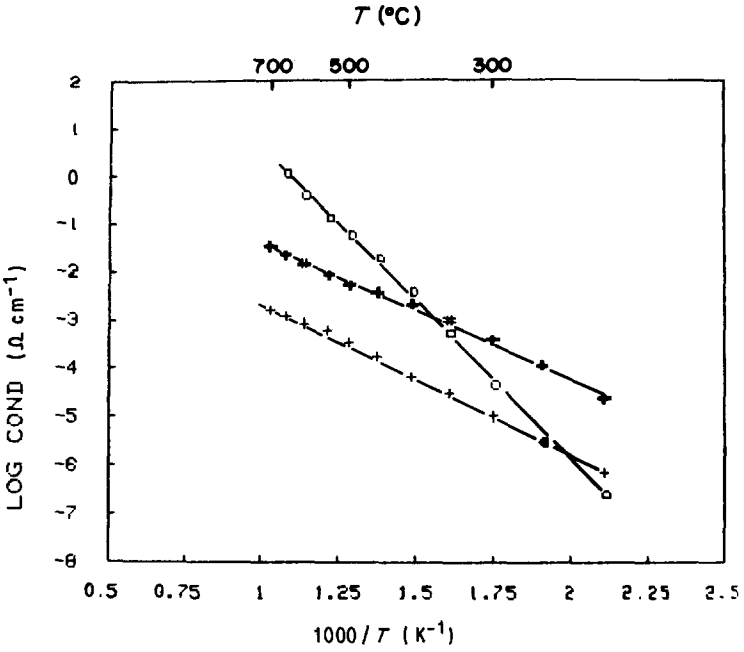

Figure 12 Log lattice conductivity plotted against temperature of various ceramic solid electrolytes. (□) Bi_2O_3–18% Er_2O_3, (+ CeO_2–8% Gd_2O_3, (+) ZrO_2–3% Y_2O_3.

temperatures was controlled by the dissociated vacancies which can migrate with a ΔH_σ = 60 kJ mol^{-1}. At lower temperatures the oxygen vacancies are trapped in complexes; for long-range migration they must be dissociated. Thus in this temperature region, ΔH_σ = 89 kJ mol^{-1}.

We have obtained electrical conductivity data using impedance plots in an extended temperature range up to 900° C and no break was noticed. Therefore, we cannot say that two temperature regions are available in our TZP samples, and it thus is impossible to estimate ΔH_m by applying the Bauerle and Hrizo [24] method. It is very difficult to explain why we have not found a break in the temperature dependence on conductivity, but one reason could be the small amount of dopant level in TZP and its uniform defect distribution throughout the tetragonal matrix, and difficulties in forming vacancy–dopant associations for the large vacancy-dopant distance expected in TZP structures, thus no significant coulombic interactions or other related events could occur.

In fluorite materials it is more likely that a break in the conductivity plots can thus appear, because the higher level of dopant concentration, the probability that a number of associated defect pairs can be formed, is increased and an almost complete association of defect pairs governs the low-temperature region, so that reported values of 0.4 to 0.5 eV for ΔH_{AI} are obviously expected in the high-temperature region, "free" and non-interacting V_0'' and Y'_{Zr} predominate and complex dissociation occurs.

In our TZP, over a wide temperature range (200 to 900° C) it would be expected that the low pair defect association does not significantly change and it can be related to the more favourable structural arrangement on the tetragonal for vacancy motion. Cormack [22] has deduced from computer simulation studies that when a vacancy is moved to the next neighbour site

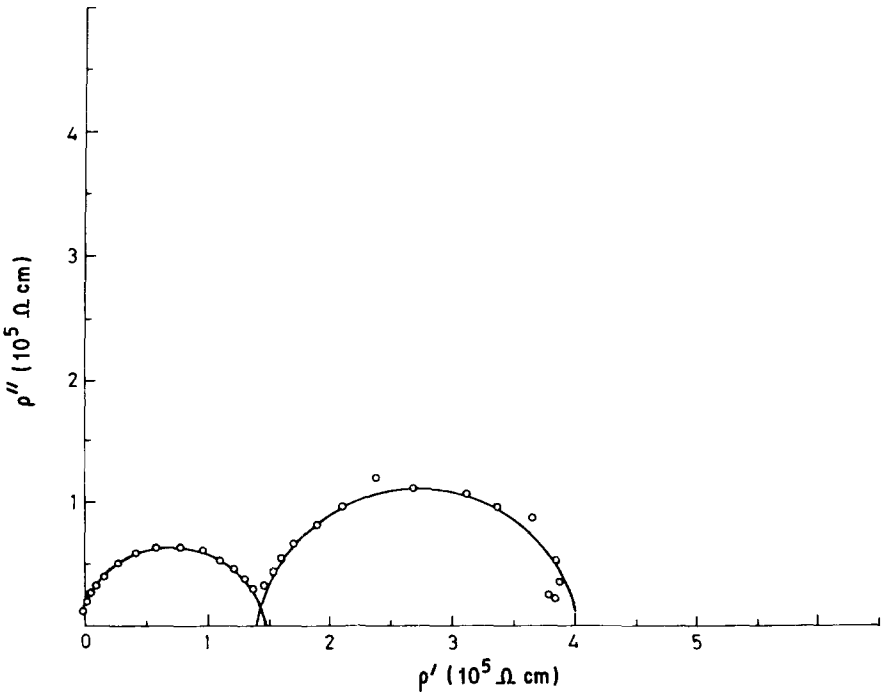

Figure 13 A.c. impedance plots of the 10 mol % CeO_2–TZP solid electrolyte ceramic; T = 325° C.

TABLE III Electrical properties of TZP-Ce samples

Material	σ_{GI} (300° C) ($S\,cm^{-1}$)	σ_{GB} (300° C) ($S\,cm^{-1}$)	ΔH_{GI} ($eV\,kJ\,mol^{-1}$)
White sample (TZP-Y1)	1.11×10^{-5}	3.41×10^{-6}	0.82–79.0
1.7Y–10CeO_2	4.77×10^{-7}	–	0.977–94
2.0Y–10CeO_2	2.42×10^{-6}	1.57×10^{-6}	1.06–102
2.5Y–10CeO_2	1.644×10^{-6}	9.03×10^{-7}	0.985–95
3Y–10CeO_2	1.95×10^{-6}	1.46×10^{-6}	1.044–100

GI = grain interior. GB = grain boundary.

configuration the tetragonal form provides a better structure than the cubic one and the association energy trends to be zero, when Y^{3+} is the dopant.

We have roughly estimated ΔH_{A1} of various TZP materials using the expression reported elsewhere [11]; the results of our calculations are given in Table IV. The association enthalpies of TZP samples are even lower than those estimated in ceria-based electrolytes where $\Delta H_{A1} \approx 0.20\,eV$ is found [25]. On the other hand, Er-TZP and Y-TZP show similar ΔH_{A1} values. This fact involves higher ΔH_m values for Er-TZP. Furthermore, the ratio of the dopant radius, r_d, to the host cation radius, r_h, are very close for Er-TZP and Y-TZP samples. Therefore, neither crystal structure nor the possible mismatch between the host and the dopant cation can explain this result. Calculations on electrical grain boundary conductivity on both type of sample [8] indicate that Y-TZP samples could agreed with the "brick layer model" whereas Er-TZP allows a different pattern. Microstructure and high ordering in the oxygen sublattice of the Er-TZP may account for its higher ΔH_m value. Although Table IV must be considered as a rough estimation, it seems to indicate that an important discrepancy related to ΔH_m values observed in the literature has been found. As a consequence it should encourage a deep discussion between workers interested in solving this disagreement. Finally when 10 mol% CeO_2 is introduced into a Y-TZP matrix a decrease in conductivity and an increase in activation enthalpy values were clearly noticed; this result can be considered, as expected [26], to be due to the fact that two host cations may induce a high pair defect associate concentration and therefore higher association enthalpy.

Acknowledgements

The authors thank Mr F. Almendros and M. Rodríguez for their contribution to the preparation of sintered materials, and Mr E. Díaz for the observation of microstructure throughout the TZP ceramic work carried out. This work was funded by the Spanish Research Council (CSIC) under contract no. 999/070.

TABLE IV Some activation enthalpies of lattice conductivity

Material	ΔH_σ (eV)	ΔH_m (eV)	ΔH_{A1} (eV)
Y-TZP	0.80	0.67	0.13
Er-TZP	0.85	0.70	0.15
PSZ	1.07	0.68	0.39
CeO_2–Gd_2O_3*	0.86	0.61	0.25
CeO_2–8% Gd_2O_3†	0.60	0.50	0.10

*[25].
†Our estimate.

References

1. P. DURÁN, P. RECIO, J. R. JURADO, C. PASCUAL and C. MOURE, *J. Mater. Sci.* **23** (1988) 0000.
2. P. DURÁN, P. RECIO, J. R. JURADO, C. PASCUAL, F. CAPEL and C. MOURE, *ibid.* **23** (1988) 0000.
3. T. K. GUPTA, R. B. GREKILA and E. C. SUBBARAO, *J. Electrochem. Soc.* **128** (1981) 929.
4. N. BONANOS, R. K. SLOTWINSKI, B. C. H. STEELE and E. P. BUTLER, *J. Mater. Sci. Lett.* **3** (1984) 245.
5. C. MOURE, J. R. JURADO, P. DURÁN, Proceedings of the British Ceramic Society no. 36, "Electric Ceramics", edited by B. C. H. Steele (Stoke-on-Trent, UK) (1985) p. 31.
6. K. KEIZER, M. VAN HEMERT, M. A. C. G. VAN DE GRAAF and A. J. BURGGRAAF, *Solid State Ionics* **16** (1985) 67.
7. J. R. JURADO, C. MOURE and P. DURÁN, in "Proceedings of the 6th Riso International Symposium, Roskilde, Denmark, September 1985", edited by F. W. Poulsen *et al.* (Odense, Denmark, 1985) p. 305.
8. J. R. JURADO, C. MOURE and P. DURÁN, *Physique* **47** (1986) C1-789.
9. K. KEIZER, M. VAN HEMERT, A. J. A. WINNUBST, M. A. C. G. VAN DE GRAAF and A. J. BURGGRAAF, *ibid.* **47** (1986) C1–783.
10. M. WELLER and H. SCHUBERT, *J. Amer. Ceram. Soc.* **69** (1986) 573.
11. C. PASCUAL, C. MOURE, J. R. JURADO and P. DURÁN, in "High Tech Ceramics", edited by Vincenzini (Elsevier, Amsterdam, 1987) p. 1915.
12. T. SATO and M. SCHIMADA, *J. Mater. Sci.* **20** (1985) 3988.
13. *Idem, Amer. Ceram. Soc. Bull.* **64** (1985) 1382.
14. K. TSUKUMA and M. SHIMADA, *J. Mater. Sci.* **20** (1985) 1178.
15. P. DUWEZ and F. ODELL, *J. Amer. Ceram. Soc.* **33** (1950) 274.
16. E. TANI, M. YOSHIMURA and S. SOMIYA, *ibid.* **66** (1983) 506.
17. J. E. BAUERLE, *J. Phys. Chem. Solids* **30** (1969) 2657.
18. C. M. MARI, *Solid State Ionics* **12** (1984) 419.
19. H. J. WON, S. H. PARK, K. H. KIM and J. S. CHOI, *J. Phys. Chem. Solids* **48** (1987) 383.
20. N. BONANOS, R. K. SLOTWINSKI, B. C. H. STEELE and E. P. BUTLER, *J. Mat. Sci.* **19** (1984) 785.
21. S. IKEDA, O. SAKURAI, K. UEMATSU, N. MIZUTANI and M. KATO, *J. Mater. Sci.* **20** (1985) 4593.
22. A. N. CORMACK, in Proceedings 6th Riso International Symposium, Roskilde, Denmark, September 1985, edited by F. W. Poulsen *et al.*, Odense, Denmark, 1985, p. 11.
23. A. N. CORMACK, in "High Tech Ceramics", edited by P. Vincenzini, (Amsterdam, 1987) p. 351.
24. J. E. BAUERLE and J. HRIZO, *J. Phys. Chem. Solids* **30** (1969) 565.
25. J. A. KILNER and B. C. H. STEELE, in "Non stoichiometric oxides", edited by O. T. Sorensen (Academic, New York, 1981) p. 233.
26. B. CALES and J. F. BAUMARD, *Rev. Int. Hautes Temp. Refract.* **17** (1980) 137.

Received 12 October 1987
and accepted 10 February 1988